Unifying Interfacial Self-Assembly and Surface Freezing

B. M. Ocko,[1,*] H. Hlaing,[1] P. N. Jepsen,[1] S. Kewalramani,[1] A. Tkachenko,[2] D. Pontoni,[3] H. Reichert,[3] and M. Deutsch[4]

[1]*Condensed Matter Physics & Materials Sciences Department, Brookhaven National Laboratory, Upton, New York 11973, USA*

[2]*Center for Functional Nanomaterials, Brookhaven National Laboratory, Upton, New York 11973, USA*

[3]*European Synchrotron Radiation Facility, P.O. Box 220, 38043 Grenoble, France*

[4]*Physics Department & Institute of Nanotechnology, Bar-Ilan University, Ramat-Gan 52900, Israel*

(Received 20 January 2011; published 30 March 2011)

X-ray investigations reveal that the monolayers formed at the bulk alkanol-sapphire interface are densely packed with the surface-normal molecules hydrogen bound to the sapphire. About 30–35 °C above the bulk, these monolayers both melt reversibly and partially desorb. This system exhibits balanced intermolecular and molecule-substrate interactions which are intermediate between self-assembled and surface-frozen monolayers, each dominated by one interaction. The phase behavior is rationalized within a thermodynamic model comprising interfacial interactions, elasticity, and entropic effects. Separating the substrate from the melt leaves the monolayer structurally intact.

DOI: 10.1103/PhysRevLett.106.137801 PACS numbers: 68.18.−g, 61.05.cm, 64.75.Yz

The wide-ranging fascination with nanoscale structures over the last decades has spurred renewed interest in the formation of single molecule thick organic layers, both for fundamental science [1,2] and for applications ranging from biosensor [3] to organic photovoltaic devices [4]. At one end of the spectrum of monolayer formation are self-assembled monolayers (SAMs), like gold-supported alkyl-thiols [1,2] and silica-supported alkyl-silanes [5], where the solution prepared monolayer formation and order are dominated by the strong headgroup-substrate interaction, reaching in some cases a few hundred kJ/mole, while the weaker chain-chain van der Waals (vdW) interactions play a more minor role in determining the structure. At the other end of the spectrum stands surface freezing, where a solid monolayer of *n*-alkane molecules forms at the free surface of their own melt over a temperature range ΔT of a few degrees above T_b, the bulk melting point [6–9]. Here the lateral vdW interaction between molecules, tens of kJ/mole, dictates the frozen monolayer's structure, while the very weak interaction of the molecules with the ''substrate'' (the vapor) plays only a minor role. These weak surface interactions, due to the higher surface affinity of the hydrogen-rich CH_3 endgroups compared with the mostly-CH_2 bulk, are predicted to be the origin of surface freezing [10,11]. No systems intermediate between these two extremes have been investigated structurally to date with Å-scale resolution. The present study investigates experimentally, and models theoretically, such a system, providing a unifying link between these two monolayer formation processes, and a deeper insight into the interfacial self-assembly of molecules.

Using Å-resolution surface-specific x-ray scattering [1,9] we study the structure of a dense monolayer of extended, surface-normal aligned, *n*-alkanol molecules ($C_nH_{2n+1}OH$, denoted here as CnOH) bound to the (0001) face of sapphire (α-Al_2O_3). The headgroup-substrate hydrogen bond, a few tens of kJ/mol strong (see below), is much weaker than the few hundred kJ/mole of a gold-bound alkyl-thiol molecule in a SAM [12], but much stronger than the CH_3-vapor interaction. Since it is comparable with the chain-chain interaction, a few tens of kJ/mole, both interactions play a significant role in influencing the monolayer's structure. In this Letter we show that a well-ordered monolayer of C18OH exists at the sapphire surface over a range of temperatures where the contacting bulk remains molten. The temperature range, ΔT, is about 10 times larger than that found at the melt-vapor interface and this extended range is a direct manifestation of the stronger interfacial interactions.

This study focuses on the buried interface between molten CnOH and sapphire, referred to hereafter as the *s-l* interface. However, complementary measurements were carried out also on the CnOH monolayer remaining on the sapphire surface after it was separated from the liquid reservoir, to which we refer as the *s-v* interface. Similar structural properties and temperature dependence were found for the two interfaces.

Although the formation of *n*-alkanol monolayers on solid surfaces had been inferred in the 1940s from reversible adsorption-desorption experiments from organic solvents [13], no temperature dependence and no molecular level structure have been determined. More recently, atomic force microscopy and photoelectron spectroscopy measurements of octadecanoic (stearic) acid on sapphire, also a system with intermediate interface-headgroup interactions, have revealed detailed information on the SAM formation process [14] and the nature of the interactions [15]. For bulk *n* alkanes in contact with sapphire only surface parallel molecules were observed at the interface and surface freezing was not observed in optical measurements [16]. In the present study, the solid monolayer which

forms on the sapphire in contact with the melt is found to remain on the sapphire after it is separated from the melt; thus, surface freezing provides a route for making well-formed SAMs.

The x-ray reflectivity (XR) measurements were carried out using 72.5 and 32 keV x rays at ID15A(ESRF) [17] and X22A (NSLS) [9] at the solid-liquid (s-l) and solid-vapor (s-v) geometries as shown in Fig. 1. A sealed sample cell, the temperature of which was controlled to 0.5 °C, contained both a reservoir filled with the CnOH melt and the cleaned sapphire (0001) crystal ($10 \times 10 \times 0.4$ mm^3), held from above by a micrometer-positioned vacuum-based sample holder. This allowed the sapphire to be placed in contact with the CnOH melt [Fig. 1(a)], while leaving a 1–2 mm gap between the reservoir's top and the sapphire. Additional XR measurements were carried out on the sapphire's surface after it was lifted off the bulk melt [Fig. 1(b)] by a few mm. In both configurations the XR was measured versus q_z, the surface-normal wave vector transfer [9], by tilting the sample cell. The critical q_c vectors [9] were 0.0356 Å^{-1} and 0.0406 Å^{-1} at the (s-l) and (s-v) interfaces, respectively.

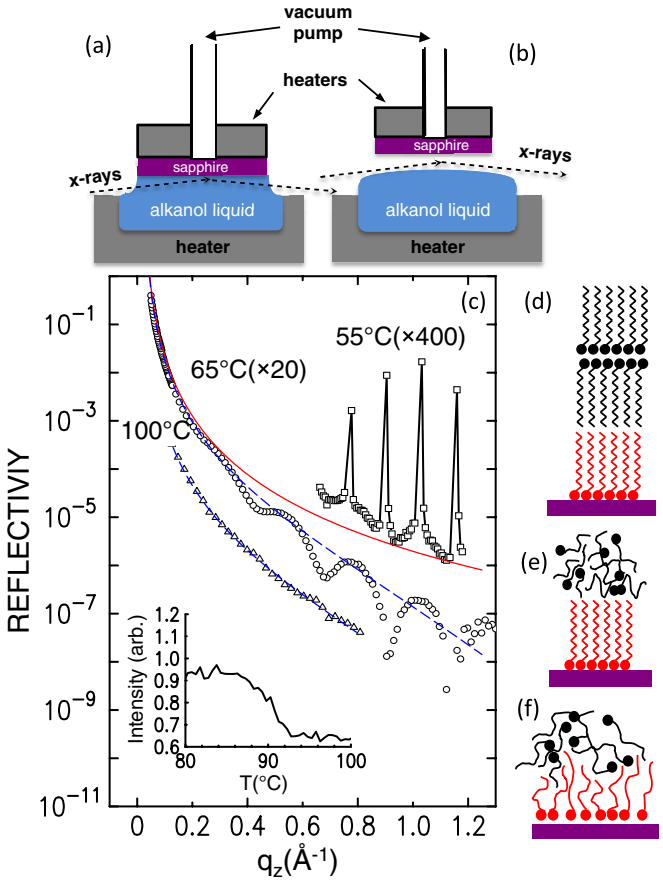

FIG. 1 (color online). (a) s-l and (b) s-v interface configurations. (c) X-ray reflectivity versus q_z at the s-l (sapphire/C18OH) interface at 55, 65 and 100 °C corresponding to the crystalline (□), monolayer (○) and disordered (△) phases. The calculated Fresnel curves are shown with no roughness (solid line) and a roughness of 1.5 Å (dashed line). (inset) Intensity at $q_z = 0.55$ Å^{-1} versus temperature exhibiting the transition between the surface-frozen monolayer and disordered phases. (d),(e),(f) Schematic descriptions of the crystalline (d), monolayer (e) and disordered (f) surface phases.

Figure 1(c) shows the XR at the C18OH/sapphire interface at several temperatures along with R_F, the theoretical reflectivity of an ideally flat and smooth interface. As shown below, these XR profiles correspond to the crystalline (d), surface monolayer (e), and disordered (f) phases shown in Fig. 1. At 55 °C (□), a temperature less than the bulk freezing point, $T_f = 59.8$ °C, Bragg Peaks are observed which correspond to a bilayer spacing of ~49 Å. Above T_f at 65 °C (○) the XR exhibits well-defined modulations whose q_z period is about twice that in the crystalline phase, indicating the formation of a dense interfacial monolayer and the absence of a bulk solid. By 100 °C (Δ) the modulations have nearly vanished suggesting that the monolayer has melted. Modeling this curve—without accounting for the small modulation in q_z—yields a near atomic perfection of the sapphire surface with a Gaussian roughness of only 1.5 Å. The melting of the monolayer is clearly visible between 87 and 92 °C, as demonstrated by the gradual intensity change which occurs in this interval (see inset to Fig. 1). The transition is reversible, albeit with a small, slew rate dependent hysteresis.

Figure 2(a) shows selected Fresnel-normalized XR curves of the monolayer phase, exhibiting well-defined Kiessig-like interference fringes of waves reflected from the monolayer's top and bottom interfaces. At the s-l interface the modulation amplitude increases with increasing q_z for both C18OH (black ○) and C12OH (blue ∇).

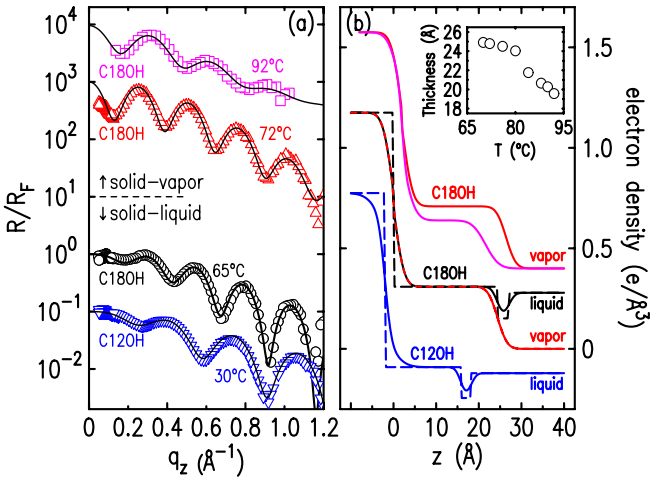

FIG. 2 (color online). (a) Measured (symbols) and model fitted (lines), Fresnel-normalized reflectivity curves, R/R_F, in the frozen monolayer phase for C12OH and C18OH at the indicated interfaces and temperatures, vertically spaced for clarity. (b) Electron density profiles corresponding to the fitted model (solid lines) and with the interfacial roughness set to zero (dashed lines). (inset) Fitted monolayer thickness versus temperature at the s-v interface.

In contrast, for the s-v C18OH-coated sapphire at 72 °C (red Δ) a nearly perfect sinusoidal modulation is observed. Although the modulations of the C18OH XR curves at the two interfaces are phase shifted from each other, they exhibit the same period of $\Delta q_z = 0.255$ Å^{-1}, corresponding to an equal layer thickness of $d_{18} = 2\pi/\Delta q_z \simeq 24.6$ Å at both interfaces. As we show below, the phase shift is due to the different top termination of the density profiles. For the C12OH monolayer at the s-l interface the modulation period is 0.35 Å^{-1}, corresponding to a spacing of $d_{12} \simeq 18.0$ Å. d_{18} and d_{12} are close to the corresponding extended molecular lengths, indicating that the molecules are standing upright. Additional measurements (not shown) for C10OH, C14OH, and C20H lead to the same conclusion. Similar XR profiles were obtained at the calcite surface in contact with stearic acid solutions in methanol by Fenter and co-workers [18].

To gain deeper insight into, and more detailed information on the structure of the interface, we constructed a ''slabs'' model for the surface-normal electron density $\rho(z)$, consisting of 4 slabs: (a) sapphire, (b) hydrocarbon monolayer, (c) depletion region between the monolayer and bulk n-alkanol and (d) bulk liquid n-alkanol. For the s-v interface the regions (c) and (d) are replaced by a zero density vapor region. Substituting this profile into the master formula [19] yields an expression for the XR curve, which is then fitted to the measured XR curve. The sapphire, monolayer, and bulk liquid electron densities were kept fixed at 1.175, 0.309, and $0.284e/$Å^3, respectively, their literature values [20] and only the interfacial roughness and thickness parameters were allowed to vary. To further reduce the number of free parameters, we have simultaneously fitted the C18OH XR curves at the s-l and s-v interfaces with the same parameters which describe the hydrogen bonded frozen monolayer. The fits, shown by the solid lines in Fig. 2(a), provide an excellent description of all measured R/R_F curves.

The corresponding density profiles, shown in Fig. 2(b), demonstrate the simple and physical nature of the model. At the s-l interface both the C12OH and C18OH exhibit a similar depletion region between the terminal methyl group of the monolayer and the bulk liquid. Without the depletion layer the model reflectivity fails to reproduce the strong modulations observed. The roughness parameters are all less than 1.9 Å. The simultaneous fit of the C18OH monolayer at the s-v and the s-l interfaces yields a single film thickness $d = 24.4 \pm 0.2$ Å and a depletion region thickness $\Delta d = 2.6$ Å. For the C12OH monolayer $d = 17.8$ Å and $\Delta d = 2.3$ Å. A separate uncertainty cannot be ascribed to Δd since Δd is strongly coupled with the depletion region electron density value [9].

A more reliable measure of the depletion is the integrated depletion, $\Gamma = \Delta\rho \times \Delta d$, where $\Delta\rho$ is the difference between the average of the monolayer and liquid phase densities and the density of the depleted region [21]. The fit yields $\Gamma = 0.37 \pm 0.03$ and $0.32 \pm 0.05\, e/$Å^2 for C18OH and C12OH, respectively. Similar depletion regions have been observed at the interface between a frozen n-alkane monolayer and its molten bulk [9] and between a self-assembled monolayer and water [21]. In these systems, as here, the depletion originates from the much bulkier CH_3 terminal group with its correspondingly lower electron density than the CH_2 midchain regions.

The very weak modulations in R at the s-l in the melted phase [see Fig. 1(c) at 100 °C] make it difficult to extract detailed, temperature dependent structural information at the buried interface. However, additional insight into the melting (freezing) of the C18OH monolayer, is provided by measurements obtained at the s-v interface. These results conclusively show a decrease in the film thickness with increasing temperature as evidenced by the normalized XR profiles [Fig. 2(a)] and the corresponding fit-derived density profiles [Fig. 2(b)] shown at 72 °C (red Δ) and at 92 °C (purple □). Compared with the 72 °C XR, the modulation amplitude at 92 °C is smaller, diminishes faster with q_z, and has a longer period. The fit-derived thickness values, shown in the inset of Fig. 2, decrease from ~25 Å for 70 °C to ~20 Å for 92 °C, a reduced thickness at 92 °C equal to $x = 20$ Å/25 Å = 0.80 relative to that of the frozen monolayer. The smaller, and faster decaying, modulations suggest a more diffuse interface at higher temperatures. The increase in the modulations period is particularly intriguing: it indicates a thickness contraction with increasing temperature, rather than the expected thermal expansion. It must have, therefore, a different origin. A plausible explanation of the thickness and electron density reductions is the gradual desorption of alkanols from the interface with increasing temperature. The reduction in both quantities implies a $\approx 30\%$ desorption of the sapphire-bound alkanol molecules at 92 °C. Together with in-plane diffraction results and our thermodynamic model, both presented below, our results strongly suggest that the lower density is accompanied by chain melting.

To render quantitative the arguments presented above, we propose a simple thermodynamic model akin to that of Leermakers and Cohen-Stuart [10] for surface freezing of alkanes. In that case the lower free energy of a CH_3 terminal layer relative to that of a CH_2 layer induces segregation of the CH_3 groups at the surface thus nucleating the frozen layer. Here the interfacial free energy per unit area is $\Delta\gamma_S = -\sigma_S[E_{\mathrm{OH}} - \Delta S(T - T_b)]$, where ΔS is the bulk melting entropy change of the equal-length n alkane, T_b is the alkane's bulk melting temperature, and E_{OH} is the excess free energy of an interface-bound OH headgroup over one in the melt. For the molten interfacial monolayer $\Delta\gamma_L = -\sigma_L[E_{\mathrm{OH}} - 3RTh^2/(2aL)]$, where the second term is the elastic penalty associated with stretching the chains [22,23], h is the layer thickness, L is the fully stretched length of the molecule, a is the Kuhn length, σ_S and $\sigma_L < \sigma_S$ are the number of interface-bound chains per unit area in the solid and liquid monolayer phases,

and R is the molar gas constant. Mass conservation imposes proportionality of the areal density of the interface-bound OH headgroups, σ_L, and the relative stretching of the chains, $x \equiv h/L$ yields $\sigma_L = x\lambda\sigma_S$, where $\lambda = \rho_L/\rho_S \approx 0.85$ is the mass density ratio of the liquid and solid alkane. Minimizing $\Delta\gamma_L$ with respect to x yields the equilibrium relative layer thickness: $x^* = \sqrt{2\alpha E_{\mathrm{OH}}/(RTn)}/3$, where $\alpha \approx 7$ is the number of carbon groups per Kuhn segment [22], and n is the number of carbons in the chain. Surface freezing occurs at $T = T^*$, determined by $\Delta\gamma_L(x^*, T^*) = \Delta\gamma_S(T^*)$. This yields $T^* = T_b + [1 - \lambda\sqrt{8\alpha E_{\mathrm{OH}}/(RTn)}/9]E_{\mathrm{OH}}/\Delta S$.

For $n = 18$ the bulk parameters of n alkanes are $\Delta S \approx 0.14$ J/mol and $T_b \approx 27\,^\circ$C [7]. The experimentally observed surface transition temperature, $T^* = 92\,^\circ$C, corresponds to $E_{\mathrm{OH}} \approx 14.5$ kJ/mol, which is consistent with the energy scale of medium-strength hydrogen bonding [24]. This E_{OH} yields a relative height of $x^* = 0.65$ for the disordered layer. This is reasonably close to the relative height of the disordered layer, 0.80, observed at the s-v interface. The discrepancy between the measured and calculated values of x^* can be attributed to the use of the simplified Gaussian model for chain elasticity and the high affinity of the CH_3 groups to the vapor interface.

At the s-v interface, the epitaxial nature of the monolayer is demonstrated by grazing incidence x-ray diffraction (GID) measurements (see supplemental material [25]). A GID peak from the 2D alkanol monolayer is observed at a surface-parallel scattering vector $q_r = 1.52 \pm 0.01$ Å^{-1} which coincides with the (1000) in-plane peak of the sapphire. It can be distinguished from the sapphire peak by a fraction-of-a-degree azimuthal rotation of the sapphire. This causes the sharp, single-crystal, sapphire peak to disappear, but preserves the broader alkanol peak, which originates in the monolayer's less-perfect 2D order. The epitaxy is not surprising since the sapphire lattice constant, 4.76 Å, is very close to the 4.83 Å lattice constant obtained for the C18OH surface-frozen monolayer that exists at the free surface of C18OH molten bulk [26]. The extended rod of scattering along q_z at the GID position, i.e., the Bragg Rod, (see supplemental material [25]) demonstrates that the molecules are aligned along the surface normal, forming a layer ~23 Å thick, close to the extended length of the C18OH molecules and the XR reflectivity derived thickness. Within the frozen monolayer temperature range the GID scattering is only weakly temperature dependent. Equivalent measurements are not possible at the s-l interface due to the much higher background.

Our results provide keen insight into the link between surface freezing and self-assembled monolayers. In contact with the molten alkanol bulk, an interfacial, frozen, standing-up "self-assembled monolayer" forms on the sapphire(0001) surface over a temperature range—30–35 °C for C18OH—where the bulk remains molten. The thickness change upon melting and the temperature range of the surface-frozen layer are consistent with a simple free energy model that only includes the OH-sapphire adsorption energy and the elastic penalty associated with stretching the chains. For self-assembled monolayers, the temperature range of surface freezing will depend on the energetics of the surface bond, the entropy change upon melting, and the availability of surface bonding sites.

Research supported by the U.S. Department of Energy, Basic Energy Sciences, by the Materials Sciences and Engineering Division (B. O., H. H., P. N. J., and S. K.) and through use of the CFN (A. T.) and the NSLS. Support by the U.S.-Israel Binational Foundation (M. D.) is greatly acknowledged. We thank the ESRF for provision of beam time and research support (D. P. and H. R.).

*ocko@bnl.gov

[1] A. Cossaro *et al.*, Science **321**, 943 (2008).
[2] C. D. Bain, J. Am. Chem. Soc. **111**, 321 (1989).
[3] J. N. Anker *et al.*, Nature Mater. **7**, 442 (2008).
[4] R. J. Kline *et al.*, Nature Mater. **5**, 222 (2006).
[5] J. Sagiv, J. Am. Chem. Soc. **102**, 92 (1980).
[6] J. C. Earnshaw and C. J. Hughes, Phys. Rev. A **46**, R4494 (1992).
[7] X. Z. Wu, E. B. Sirota, S. K. Sinha, B. M. Ocko, and M. Deutsch, Phys. Rev. Lett. **70**, 958 (1993).
[8] X. Z. Wu *et al.*, Science **261**, 1018 (1993).
[9] B. M. Ocko *et al.*, Phys. Rev. E **55**, 3164 (1997).
[10] F. A. M. Leermakers and M. A. Cohen Stuart, Phys. Rev. Lett. **76**, 82 (1996).
[11] E. B. Sirota, X. Z. Wu, B. M. Ocko, and M. Deutsch, Phys. Rev. Lett. **79**, 531 (1997).
[12] D. J. Lavrich, S. M. Wetterer, S. L. Bernasek, and G. J. Scoles, J. Phys. Chem. B **102**, 3456 (1998).
[13] W. C. Bigelow, D. L. Pickett, and W. A. Zisman, J. Colloid Interface Sci. **1**, 513 (1946).
[14] C. E. Taylor and D. K. Schwartz, Langmuir **19**, 2665 (2003).
[15] M. S. Lim *et al.*, Langmuir **23**, 2444 (2007).
[16] M. S. Yeganeh, Phys. Rev. E **66**, 041607 (2002).
[17] M. Mezger *et al.*, Science **322**, 424 (2008).
[18] P. Fenter and N. C. Sturchio, Geochim. Cosmochim. Acta **63**, 3145 (1999).
[19] P. S. Pershan and J. Als-Nielsen, Phys. Rev. Lett. **52**, 759 (1984).
[20] M. Deutsch *et al.*, Europhys. Lett. **30**, 283 (1995).
[21] B. M. Ocko, A. Dhinojwala, and J. Daillant, Phys. Rev. Lett. **101**, 039601 (2008).
[22] P. J. Flory, *Statistical Mechanics of Chain Molecules* (Interscience Publishers, New York, 1969).
[23] S. Alexander, J. Phys. (Paris) **38**, 983 (1977).
[24] G. R. Desiraju, Acc. Chem. Res. **35**, 565 (2002); T. Steiner, Angew. Chem., Int. Ed. **41**, 48 (2002); D. Chandler, Nature (London) **437**, 640 (2005).
[25] See supplemental material at http://link.aps.org/supplemental/10.1103/PhysRevLett.106.137801 for in-plane scattering.
[26] O. Gang, X. Z. Wu, B. M. Ocko, E. B. Sirota, and M. D. Deutsch, Phys. Rev. E **58**, 6086 (1998).